ANTIMICROBIAL AGENTS AND CHEMOTHERAPY, Dec. 2005, p. 4942–4949 Vol. 49, No. 12
0066-4804/05/$08.00+0 doi:10.1128/AAC.49.12.4942–4949.2005

Structure-Guided Discovery of Novel Aminoglycoside Mimetics as Antibacterial Translation Inhibitors

Yuefen Zhou,[1] Vlad E. Gregor,[1]† Zhongxiang Sun,[1] Benjamin K. Ayida,[1] Geoffrey C. Winters,[1]‡ Douglas Murphy,[1] Klaus B. Simonsen,[1]§ Dionisios Vourloumis,[1]¶ Sarah Fish,[1] Jamie M. Froelich,[1] Daniel Wall,[1]* and Thomas Hermann[2]*

Anadys Pharmaceuticals, San Diego, California,[1] and Department of Chemistry and Biochemistry, University of California—San Diego, La Jolla, California[2]

Received 17 August 2005/Returned for modification 30 September 2005/Accepted 4 October 2005

We report the structure-guided discovery, synthesis, and initial characterization of 3,5-diamino-piperidinyl triazines (DAPT), a novel translation inhibitor class that targets bacterial rRNA and exhibits broad-spectrum antibacterial activity. DAPT compounds were designed as structural mimetics of aminoglycoside antibiotics which bind to the bacterial ribosomal decoding site and thereby interfere with translational fidelity. We found that DAPT compounds bind to oligonucleotide models of decoding-site RNA, inhibit translation in vitro, and induce translation misincorporation in vivo, in agreement with a mechanism of action at the ribosomal decoding site. The novel DAPT antibacterials inhibit growth of gram-positive and gram-negative bacteria, including the respiratory pathogen *Pseudomonas aeruginosa*, and display low toxicity to human cell lines. In a mouse protection model, an advanced DAPT compound demonstrated efficacy against an *Escherichia coli* infection at a 50% protective dose of 2.4 mg/kg of body weight by single-dose intravenous administration.

About half of all chemical classes of antibiotics affect bacterial translation by binding to the ribosome and thereby interfering with protein synthesis. The bacterial ribosome is a key target for naturally occurring antibiotics, including the macrolides, tetracyclines, chloramphenicol, and aminoglycosides, as well as the recently discovered synthetic oxazolidinones (8, 30). Over the past 5 years, structural analyses of the ribosome, its components, and drug complexes thereof have revealed that antibiotics interact predominantly with the rRNA (1). Indeed, bacterial ribosomes contain the only validated RNA targets for which approved drugs are currently available. Aminoglycosides were among the first antibiotics for which direct interaction with rRNA was demonstrated, initially by biochemical methods and later by structural studies (25).

Aminoglycoside antibiotics, such as paromomycin and gentamicin, target the ribosomal decoding site within 16S rRNA, where they bind to an internal loop structure that is involved in maintaining translational fidelity (Fig. 1A and B). Upon association with the decoding-site loop, aminoglycosides reduce the energetic cost of a conformational transition in the ribosome that is required for monitoring the accurate match between the mRNA codon and the anticodon of cognate aminoacylated tRNA (18). The availability of three-dimensional structural information on aminoglycoside-RNA complexes has spurred efforts to design novel improved ligands for the decoding-site target to overcome limitations of the natural drugs that suffer from widespread bacterial resistance, low bioavailability, and toxicity (9, 13, 14, 24).

Here, we report the structure-guided discovery of a novel chemical class of antibacterial translation inhibitors that were conceived as mimetics of the natural aminoglycoside antibiotics. Information derived from crystal structures of aminoglycoside-RNA complexes was used to design synthetic molecule classes that contained structural features required for RNA recognition by the natural drugs. As a result of this effort, we identified 3,5-diamino-piperidinyl triazines (DAPT) (Fig. 1D and Table 1) as antibacterial agents that target the bacterial decoding-site RNA in vitro and inhibit bacterial growth by a translation-dependent mechanism.

MATERIALS AND METHODS

Reagents. Antibiotics were purchased from Sigma (St. Louis, MO). Decoding-site RNA for calorimetry experiments and fluorescence binding assays was prepared by annealing gel-purified complementary oligonucleotides purchased from Dharmacon Research (Lafayette, CO). RNA annealing was performed by heating in buffer at 75°C for 1 min, followed by snap cooling on ice.

Strains. All strains used for MIC testing are listed in Table 2 and were obtained from the American Type Culture Collection. *Escherichia coli* strains CSH102, CSH103, CSH104, and CSH105, used for the misincorporation experiments, were obtained from Jeffrey H. Miller, UCLA (16).

Chemical synthesis. Reaction conditions for the synthesis of DAPT compounds 1a to 1i (Fig. 1D and Table 1) and their precursors (Fig. 2) and their characterization will be reported elsewhere.

ITC. Isothermal titration calorimetry (ITC) experiments were performed at 25°C on a MicroCal VP-ITC instrument (MicroCal, Northampton, MA). The buffer for both the RNA target (see Fig. 3C) and the compounds was 10 mM 2-morpholinoethanesulfonic acid buffer (pH 6.7) that contained 60 mM NaCl and 0.1 mM EDTA. For a typical titration, 10-μl aliquots of 25 or 200 μM compound solution were injected into a 5-μM RNA solution. Each experiment was accompanied by a control titration in which compound solution was injected into buffer alone under identical conditions. The duration of each injection was

* Corresponding author. Mailing address: Department of Chemistry and Biochemistry, University of California—San Diego, 9500 Gilman Drive 0358, La Jolla, CA 92093-0358. Phone for Thomas Hermann: (858) 534-4467. Fax: (858) 534-0202. E-mail: tch@ucsd.edu. Phone for Daniel Wall: (858) 530-3711. Fax: (858) 530-3644. E-mail: dwall@anadyspharma.com.

† Present address: ChemBridge Research Laboratories, San Diego, Calif.

‡ Present address: QLT, Inc., Vancouver, British Columbia, Canada.

§ Present address: H. Lundbeck A/S, Valby, Copenhagen, Denmark.

¶ Present address: National Centre for Scientific Research "Democritos," Athens, Greece.

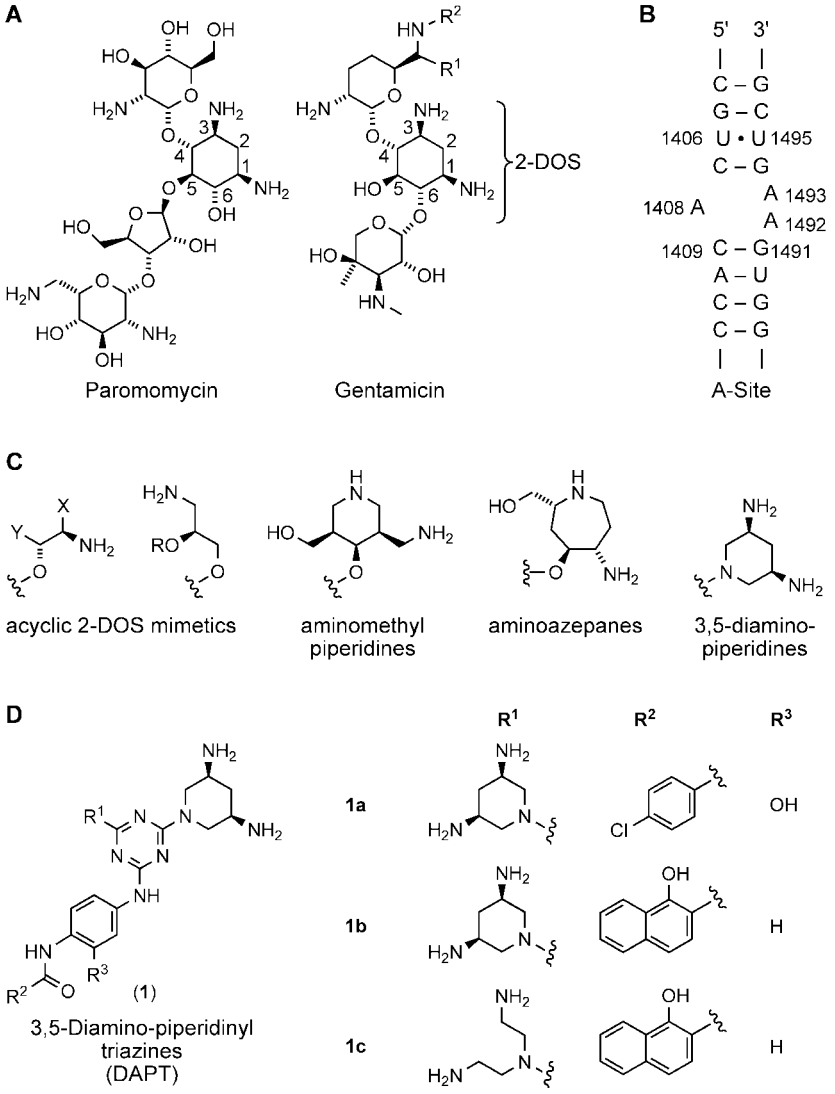

FIG. 1. (A) Natural aminoglycoside antibiotics that target the bacterial ribosomal decoding site. The natural products are derived from 2-DOS by glycosidic substitutions at positions 4 and 5 (paromomycin) or 4 and 6 (gentamicin). Gentamicin is a mixture of gentamicin C1 ($R^1 = R^2 = CH_3$), gentamicin C1A ($R^1 = R^2 = H$), and gentamicin C2 ($R^1 = CH_3$, $R^2 = H$). (B) Secondary structure of the bacterial decoding site (A-site) within 16S rRNA. Residues that are involved in aminoglycoside interactions are labeled. (C) Scaffolds that were designed and studied as structural mimetics of the aminoglycoside 2-DOS core (2, 22, 28). 3,5-Diaminopiperidines are described in this report. (D) Structure of DAPT antibacterials (compounds designated by the number 1). Compounds 1a to 1c contain at least one *cis*-3,5-diamino-piperidinyl group.

10 s, and the delay between injections was 240 s. Analysis of ITC curves by integration and buffer correction was performed using ORIGIN software (MicroCal).

Decoding-site fluorescence binding assay. Compounds were tested for binding to the decoding-site target by using an RNA fluorescence assay (20) which determines the binding affinity of a ligand based on its ability to quench or enhance emission of a fluorescent label attached at the positions of the flexible adenines A1492 or A1493 upon association with a model oligonucleotide (Fig. 3C). Fluorescence measurements were performed with 3-methylisoxanthopterin (3-MI)-labeled decoding-site RNA in cacodylate buffer (30 mM, pH 6.8) on an RF-5301PC spectrofluorometer (Shimadzu, Columbia, MD) at 25°C. Emission spectra were recorded at a 1-μM RNA concentration in 1-cm-path-length quartz cells. The excitation wavelength was at 350 nm, while emission was monitored at 430 nm. Complete experimental details of the assay have been reported elsewhere (20).

Bacterial in vitro transcription-translation assay. Test compounds were incubated in a 384-well plate with bacterial S30 extract (Promega, Madison, WI), followed by addition of a mixture of nucleotide triphosphates, amino acids, and pBEST*luc* plasmid DNA (Promega) encoding the luciferase reporter (20 μl final reaction volume). Plates were incubated at 25°C for 20 min. After the mixture was cooled on ice, SteadyGlow luciferin substrate (Promega) was added, followed by incubation for 15 min at room temperature. Light emission from the plates was recorded with a TopCount luminescence counter (Perkin Elmer, Wellesley, MA). Each compound was tested in a dose-response fashion at concentrations ranging from 1 mM to 100 nM. Values of 50% inhibitory concentration (IC_{50}) were determined from light units versus log(concentration) plots fit to a variable-slope dose-response equation. Six replicate experiments were run per concentration. To rule out inhibition of the bacterial RNA polymerase or firefly luciferase reporter enzyme, selected DAPT compounds were counter-screened against polymerase and luciferase.

Antibacterial susceptibility determination (MIC). Bacterial strains were tested in Mueller-Hinton broth by the microdilution method as described by the National Committee for Clinical Laboratory Standards (17).

Eukaryotic cytotoxicity assay. Eukaryotic cytotoxicity of compounds was assessed with a proliferation assay measuring the mitochondrial reduction of 2, 3-bis(2-methoxy-4-nitro-5-sulfophenyl)-5-[(phenyl-amino)carbonyl]-2*H*-tetrazolium hydroxide (XTT) into an orange formazan dye by CEM T cells (5). After cells were incubated with series of compound concentrations for 72 h, XTT

TABLE 1. Structure-activity relationships for DAPT compounds[a]

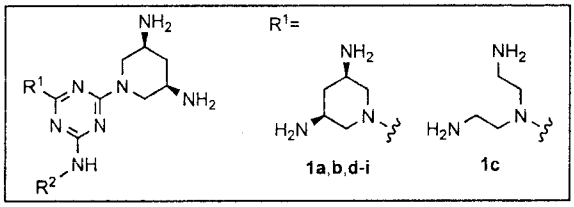

Compound or aminoglycoside	R^2	IC_{50} (μM)[b]	MIC (μg/ml)[c]	CC_{50} (μM)[d]
1d	H	92	>64 / >64	12
1e	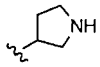	36	>64 / >64	20
1f	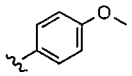	21	>64 / >64	12
1g	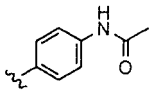	11	64 / 64	120
1h	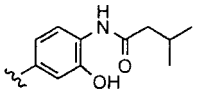	12	16 / 32	140
1i	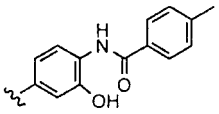	7	4 / 64	160
1a	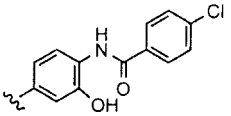	7	2 / 16	180
1b	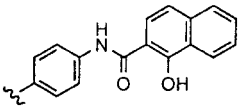	10	1 / 2	140
1c		10	4 / 8	170
Paromomycin		0.23	4 / 0.5	>300
Gentamicin		ND[e]	<0.5 / <0.5	>300

[a] For structures of 1c and the aminoglycosides paromomycin and gentamicin, see Fig. 1D. For experimental details, see Materials and Methods.
[b] IC_{50} values were determined by a coupled transcription-translation assay using *E. coli* extract.
[c] MICs are for *E. coli* ATCC 25922 (first value) and *S. aureus* ATCC 25923 (second value).
[d] Eukaryotic cytotoxicity (CC_{50}) was determined with CEM T cells.
[e] ND, not determined.

solution was added and fluorescence was read at 450 nm and 650 nm. The 50% cytotoxic concentration (CC_{50}) was determined as the compound concentration required to reduce by 50% the number of viable cells.

Test of concentration-dependent bactericidal activity. *Pseudomonas aeruginosa* strain ATCC 27853 was grown to early log phase in Mueller-Hinton broth at 37°C. The culture was diluted to 5×10^5 CFU/ml in fresh media containing various concentrations of DAPT compound 1b (1 to 64 μg/ml). Samples were then collected at various times, serially diluted, and plated. After overnight growth, viable colonies were counted.

Test of translation-dependent bactericidal activity. The method used to access bacterial killing has been described previously (15). Briefly, *E. coli* strain MG1655 was grown in Mueller-Hinton broth to mid-log phase and then diluted 10,000-fold into fresh prewarmed media. As indicated, prior to the addition of test compound, cultures were preincubated with chloramphenicol (20 μg/ml) for 5 min at 37°C. Test antibiotics gentamicin, polymyxin B, and 1a were added at 64-fold above MICs. Aliquots from each treatment tube were removed at the indicated times, serially diluted, plated, and incubated overnight at 37°C. CFU were counted, and the CFU/ml was calculated.

Translation misincorporation assay. *E. coli* strains CSH102, CSH103, CSH104, and CSH105 each contain a different mutation in the active-site glutamate residue of β-galactosidase (16). In these strains, codon 461 has been changed to, respectively, GGG (glycine), CAG (glutamine), GCG (alanine), or GTG (valine). To assay for misincorporation, triplicate cultures were grown in Luria broth over a range of compound concentrations. The concentration of compound that allowed an unshaken overnight culture to reach an optical density at 600 nm of approximately 0.3 was chosen for analysis (23). β-Galactosidase assays were done as described by Miller (16). The degree of misincorporation was defined by the increase in activity compared to that of the no-additive control.

In vivo efficacy testing. A lethal dose (2.5×10^8 CFU/mouse) of *E. coli* ATCC 25922 was used to induce systemic infection in mice by the intraperitoneal (i.p.) route. For these studies, male BALB/c mice of 5 to 6 weeks of age (20 to 22 g)

TABLE 2. Antibacterial spectra of DAPT compounds and gentamicin as a control

Organism	Strain	Resistance phenotype[b]	MIC (μg/ml) of:			
			1a	1b	1c	Gentamicin
E. coli	ATCC 25922		2	1	4	<0.5
	MG1655		1	<0.5	4	<0.5
P. aeruginosa	ATCC 27853		<0.5	1	1	<0.5
	ATCC 39324[a]		4	4	2	<0.5
	ATCC 51674[a]		1	1	8	<0.5
	ATCC 25619[a]		<0.5	<0.5	2	<0.5
	BAA-47		<0.5	0.5	2	<0.5
Enterobacter cloacae	ATCC 23355	Bla^r	2	1	4	<0.5
Klebsiella oxytoca	ATCC 51983	Bla^r	2	1	4	4
Haemophilus influenzae	ATCC 49247		>64	>64	ND[c]	2
Burkholderia cepacia	ATCC 25416		>64	>64	>64	16
Bacillus cereus	ATCC 14579		32	8	32	1
Bacillus thuringiensis	ATCC 33679		64	32	64	2
S. aureus	ATCC 25923		16	2	8	<0.5
	BAA-38[a]	Met^r Pen^r Str^r Tet^r	16	8	16	<0.5
	BAA-40[a]	Met^r Spt^r	32	8	16	>64
	BAA-44[a]	Amp^r Ery^r Gen^r Met^r Oxa^r Pen^r Tet^r	32	8	16	>64
Enterococcus faecalis	ATCC 29212		>64	>64	>64	8
	ATCC 51299	Van^r	>64	>64	32	>64

[a] Clinical isolate.
[b] Amp, ampicillin; Bla, β-lactams; Ery, erythromycin; Gen, gentamicin; Met, methicillin; Oxa, oxacillin; Pen, penicillin; Spt, spectinomycin; Str, streptomycin; Tet, tetracycline; and Van, vancomycin.
[c] ND, not determined.

were chosen. Each group contained 10 mice, and each mouse was dosed with DAPT compound by the intravenous (i.v.) route 1 h postinoculation. Compound 1c was formulated in a 140-mM sodium acetate buffer (pH 5.5). Mice were then monitored for 7 days. These studies were conducted as contracted research by NAEJA Pharmaceutical, Inc. (Edmonton, Alberta, Canada), in compliance with all standard procedures for use of animals in research.

RESULTS AND DISCUSSION

Design and synthesis of DAPT compounds. In the past, our group has extensively used three-dimensional structure data of aminoglycoside decoding-site complexes for the design and synthesis of novel RNA-targeted ligands based on fragments of the natural products (2, 21, 22, 27–29). Studies of semisynthetic aminoglycoside mimetics in our laboratory, along with findings published by others (26), have led us to identify 2-deoxystreptamine (2-DOS) (Fig. 1A) as a key pharmacophore of the natural aminoglycosides. In previous work, we designed simplified structural mimetics of the 2-DOS scaffold to reduce the complexity of the natural products and to facilitate synthesis of aminoglycoside mimetics (Fig. 1C) (2, 22, 28). The *cis*-3,5-diamino-piperidinyl (DAP) moiety, which retains the signature *cis*-1,3-diamino fragment of 2-DOS while disposing of additional stereocenters, proved to be a particularly suitable building block for RNA-targeted small-molecule libraries. The DAP scaffold possesses an intrinsic *meso*

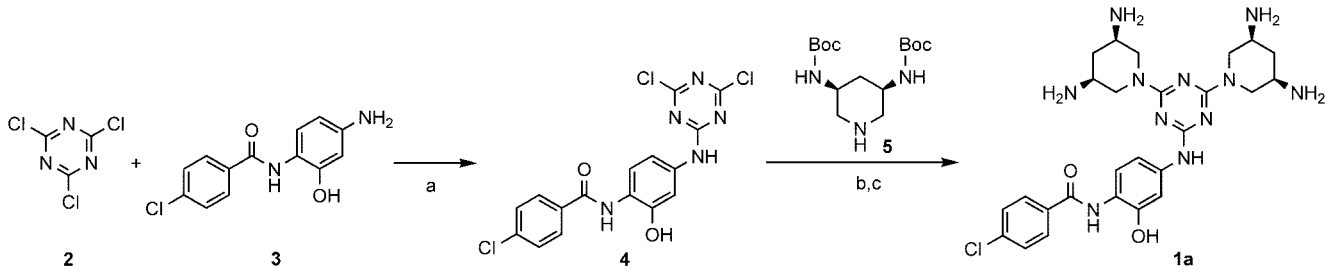

FIG. 2. Exemplary synthesis of a DAPT compound (1a) starting from 1,3,5-trichloro-triazine (marked by the number 2). Reagents and conditions are as follows: (a) diisopropyl-ethyl amine ($^i Pr_2NEt$) and tetrahydrofuran (THF); −25°C, 12 h; (b) $^i Pr_2NEt$ and THF; 80°C, 48 h; (c) HCl, 1,4-dioxane, and methanol; room temperature, 12 h. Syntheses of anilide (marked by 3) and protected 3,5-diamino-piperidine (marked by 5) as well as those of other DAPT compounds will be reported elsewhere. Boc, tert-butoxycarbonyl.

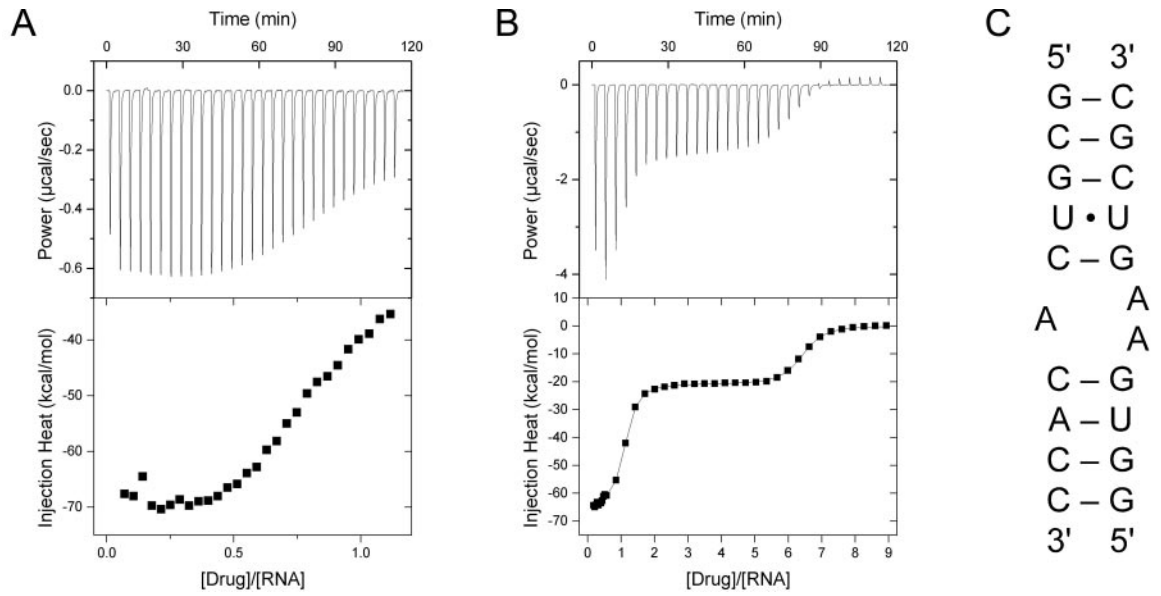

FIG. 3. ITC of the interaction of DAPT compound 1b with an oligonucleotide representing the bacterial decoding site (for experimental details, see Materials and Methods). (A) ITC trace (top) and integrated curve (bottom) for the initial binding events at low ligand concentration (25 μM ligand, 5 μM RNA). (B) ITC trace (top) and integrated curve (bottom) for the saturating titration (200 μM ligand, 5 μM RNA) merged with the titration at low ligand concentration. Binding parameters were calculated from fitting a two-site binding model to the integrated curve. Results for site 1: K = $(2.0 \pm 0.2) \times 10^9$ M^{-1}; $\Delta H = -64 \pm 0.4$ kcal/mol; stoichiometry = 1.00 ± 0.01. Results for site 2: K = $(1.3 \pm 0.1) \times 10^7$ M^{-1}; $\Delta H = -21 \pm 0.1$ kcal/mol; stoichiometry = 5.28 ± 0.01. K, binding constant; ΔH, binding enthalpy. (C) Secondary structure of the RNA target used for ITC experiments.

symmetry, reducing the complexity of stereoisomer formation during synthesis, and is readily linked to other groups via an achiral nitrogen atom.

Among the different classes of DAP derivatives that we studied, a series of symmetrically substituted DAPT proved to be amenable to optimization based on structure-activity relationship data (Table 1). The triazine core provided access to a straightforward synthetic route (Fig. 2) that contained two DAP scaffolds in a desirable stereochemical orientation that we identified in our modeling studies. Elaboration of the DAPT series produced numerous biologically active molecules, among them the representative compounds 1a, 1b, and the asymmetrically substituted triazine 1c (Fig. 1D and Table 1) (31). The following sections outline experiments conducted with these subseries representatives, producing results that were typical for the general DAPT series.

RNA target binding of DAPT compounds. To test DAPT compounds for binding to the decoding-site target, we used a fluorescence assay and isothermal titration calorimetry. Structural studies of decoding-site RNA-aminoglycoside complexes have demonstrated that small oligonucleotides can accurately reproduce the natural state of the decoding site bound to antibiotics as seen within the whole 30S subunit and, therefore, provide authentic and readily accessible models (26). Additional validation of the use of oligonucleotide models for the decoding site is provided by fluorescence experiments that probed the conformational flexibility of the unpaired adenine residues 1492 and 1493 (Fig. 1B), which are locked in one state upon binding of aminoglycoside antibiotics (4). RNA constructs of the decoding-site sequence that have either A1492 or A1493 replaced by fluorescent bases such as 2-aminopurine or 3-MI can be used to monitor ligand binding by measuring fluorescence quenching or enhancement upon titration with a potential binder (12, 20). While these experiments do not necessarily reveal the exact binding place or orientation of a ligand, interaction in an aminoglycoside-like fashion can be surmised as long as RNA complex formation induces a change in the chemical environment of the fluorescent base. We used our RNA fluorescence assay (20) to assess target interaction of DAPT compounds. The results suggested that 1a, 1b, and 1c bind with <1 μM affinity to a 3-MI-labeled oligonucleotide containing the bacterial decoding-site sequence. Precise quantitation of the binding affinity was not possible due to optical interference of the aromatic DAPT compounds with the emission signal of the fluorescent label.

To obtain an independent quantitative measure of DAPT binding to the decoding site, we performed ITC, adding 1b to an unlabeled RNA construct as a target (Fig. 3). Similar ITC experiments have been used to investigate aminoglycoside binding to the decoding site (10, 11, 19). These studies further support oligonucleotides as authentic models of the ribosomal decoding site. Our ITC experiments, which adopted buffer conditions optimized for the aminoglycoside-RNA interaction (10, 19), confirmed high-affinity binding of 1b to decoding-site RNA (Fig. 3). The integrated ITC data were readily fitted to a model of two independent sets of binding sites with distinct affinity and stoichiometry. The highest-affinity binding site corresponded to the complex formation of one DAPT ligand with one RNA target molecule ($n = 1$) at a K_D of 2 nM. These data suggest tight RNA binding of the DAPT compound 1b, which is comparable to the most potent aminoglycosides whose binding abilities have been measured by ITC (10, 19). The high

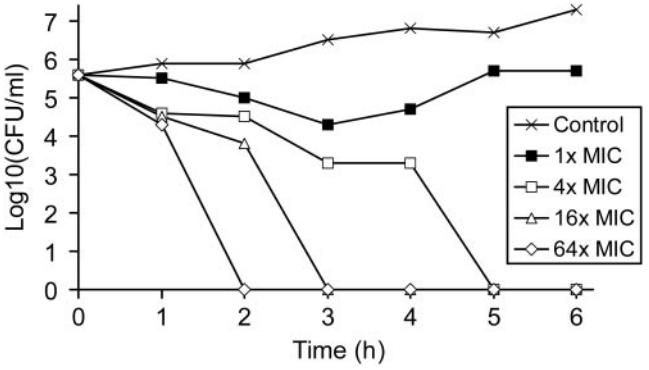

FIG. 4. Concentration-dependent bactericidal activity of DAPT compound 1b. Viability of *P. aeruginosa* ATCC 27853 was tested after exposure to increasing concentrations (1- to 64-fold over MIC) of 1b (for experimental details, see Materials and Methods). The MIC of 1b against this strain is 1 μg/ml (see Table 2).

affinity of 1b for the decoding-site RNA along with the presence of a second set of lower-affinity sites within the model oligonucleotide raises the possibility of nonspecific binding to other cellular RNA targets. Similarly, target promiscuity is well documented for RNA binding aminoglycosides, specifically neomycin (25), which is less problematic for the therapeutic use of aminoglycosides since eukaryotic cells are impermeable to these cationic drugs (24). The extent of nonspecific binding of the DAPT compounds and their potential consequences for eukaryotic compound toxicity will have to be addressed by future studies. Cytotoxicity measurements of DAPT compounds suggest however that, as with the aminoglycosides, off-target effects may have only limited impact (see below).

In vitro activity of DAPT compounds. Biological activity of DAPT compounds was assessed in vitro by testing inhibition of a cell-free bacterial transcription-translation assay with *E. coli* S30 extract and a luciferase reporter plasmid. As a control, bacterial RNA polymerase and luciferase enzyme were assayed. DAPT compounds showed inhibition of the translation assay (IC_{50}) at low micromolar concentrations (Table 1) but were inactive against the control enzymes (data not shown). The DAPT compounds were 30- to 40-fold less potent than the aminoglycoside paromomycin, which had an IC_{50} (230 nM) comparable to published values (6, 7).

Antibacterial potency of DAPT compounds was routinely measured by MIC against standard strains of *E. coli* and *Staphylococcus aureus*. While symmetrical decoration of the triazine core with two DAP moieties yielded compounds active against cell-free translation, an additional aromatic substituent was required to confer reasonable in vitro antibacterial activities (Table 1). Structure-activity relationship data derived from the in vitro translation assay in combination with MICs were used to direct compound improvement, as outlined briefly for the anilide series that led to compounds 1a, 1b, and 1c. Such optimized DAPT compounds showed MICs against *E. coli* comparable or superior to those of the aminoglycoside paromomycin but weaker than those of gentamicin (Table 1).

In vitro specificity of DAPT compounds for bacterial targets was assessed by testing cytotoxicity against eukaryotic CEM T cells (CC_{50}). A standard cell proliferation assay revealed potential for eukaryotic cytotoxicity for the symmetrically bi-

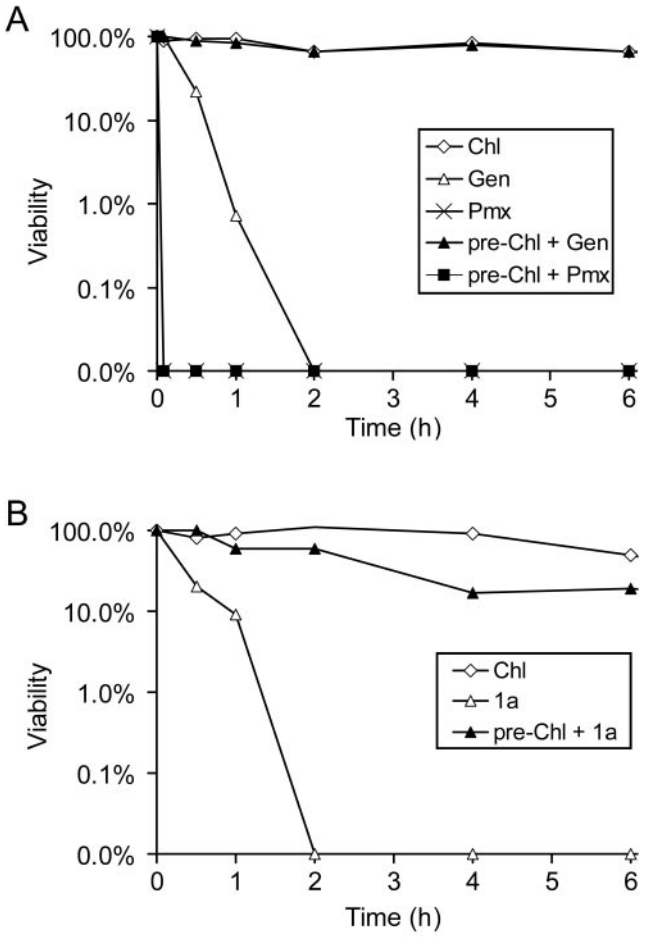

FIG. 5. Translation-dependent bactericidal activity of DAPT compound 1a (for experimental details, see Materials and Methods). (A) Control experiments with the misincorporating aminoglycoside gentamicin (Gen) and the translation-independent membrane-targeting antibacterial polymyxin B (Pmx). Both gentamicin and polymyxin B rapidly kill bacteria. Chloramphenicol (Chl) is a bacteriostatic agent. Preincubation with chloramphenicol (pre-Chl) blocks translation and hence prevents misincorporation and killing caused by gentamicin. The bactericidal action of polymyxin B is not affected by chloramphenicol preincubation. (B) Antibacterial action of the DAPT compound 1a is prevented by preincubation with chloramphenicol, similarly to the gentamicin behavior, while 1a alone kills bacteria rapidly. Compound concentrations: chloramphenicol, 20 μg/ml; gentamicin and polymyxin B, 16 μg/ml; 1a, 32 μg/ml.

substituted triazine core (Table 1, compound 1d). This problem was successfully addressed by aromatic scaffold extensions at the third substituent on the triazine core, which resulted in less cytotoxic compounds of the anilide series. The molecular causes for the cytotoxicity and the beneficial effect of the aromatic extension are not clear.

Antibacterial spectrum of DAPT compounds. After target binding and in vitro translation assays indicated that DAPT compounds were likely to interfere with bacterial protein synthesis, we studied the antibacterial activities of selected molecules. Testing of DAPT compounds against standard strains of *E. coli* and *S. aureus* during elaboration of several chemical subseries revealed a general tendency for better activity against the gram-negative organism. This trend was supported by the

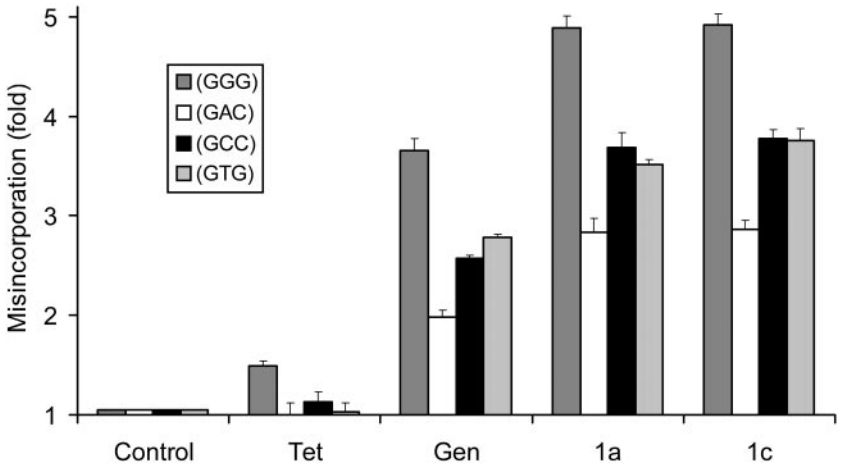

FIG. 6. Translation misincorporation induced by DAPT compounds 1a and 1c. Misincorporation of a missense mutation within an active-site residue of β-galactosidase was measured in isogenic strains of *E. coli* (for experimental details, see Materials and Methods). Four missense mutations within codon 461 were tested (see inset). The signal for untreated cells (Control) was normalized to 1. The translation inhibitor tetracycline (Tet) and misincorporating aminoglycoside gentamicin (Gen) were used, respectively, as negative and positive controls. Error bars were calculated from three independent experiments. Compound concentrations: tetracycline, 0.25 μg/ml; gentamicin, 2 μg/ml; and DAPT, 0.5 μg/ml.

assessment of selected DAPT compounds for antibacterial activity in a broader spectrum of strains (Table 2). The advanced DAPT compounds 1a and 1b were most potent against *E. coli* and *P. aeruginosa*, showing MICs comparable to or slightly above those of gentamicin. Importantly, several clinical isolates of the respiratory tract pathogen *P. aeruginosa* were susceptible for DAPT compounds. While activity against gram-positive organisms was generally weaker, 1a and 1b retained antibacterial potency against multidrug-resistant *S. aureus*, including strains that carried aminoglycoside resistance (BAA-40 and BAA-44).

Mechanistic studies of DAPT antibacterial activity. To study similarities of the antibacterial activity of DAPT compounds with that of aminoglycosides, we tested the concentration dependence of the bactericidal action over a range from 1- to 64-fold over the MIC (Fig. 4). Bacterial killing was accelerated with increasing DAPT concentration, which is comparable to the concentration-dependent killing of aminoglycosides (15). Also, growth experiments with *P. aeruginosa* (ATCC 27853), in which the DAPT concentration was reduced 1,000-fold below the MIC following a 2-h incubation, showed a 1- to 2-h postantibiotic effect on cell growth (data not shown).

Investigations of rRNA target binding and inhibition of in vitro translation were in agreement with the conception of the DAPT compounds as ligands directed at the bacterial ribosome. To further investigate whether DAPT compounds exert antibacterial activity via interference with bacterial protein synthesis in vivo, we tested whether their bactericidal activity was translation dependent (Fig. 5). In an established assay (15), bacteria whose ribosomes were blocked by chloramphenicol from synthesizing protein were incubated with 1a. Over a time course of 6 h, viable colonies were obtained from the chloramphenicol-blocked organisms, while bacteria with translating ribosomes (no chloramphenicol) were rapidly killed by the DAPT compound (Fig. 5B). The aminoglycoside gentamicin showed similar behavior (Fig. 5A). Temporary arrest of protein synthesis by chloramphenicol prevents the misincorporating action of aminoglycosides and presumably the DAPT compounds, which exert translation-dependent bactericidal activity by stimulating synthesis of erroneous proteins. In contrast, polymyxin B, which acts on the bacterial membrane and not the ribosome, retains its activity against bacteria preincubated with chloramphenicol (Fig. 5A).

To test if in vivo interaction of DAPT compounds with the bacterial ribosome involves the decoding site, which is consistent with the molecular-design concept, we measured the stimulation of misincorporation by 1a and 1c in four isogenic strains of *E. coli* (Fig. 6). These strains carried different missense mutations in an active-site residue of β-galactosidase (16). Misincorporation at the mutated codon enhances production of functional reporter enzyme. The control antibiotic tetracycline, which targets the ribosome but does not interfere with translation fidelity (3), does not stimulate misincorporation. In contrast, the aminoglycoside gentamicin and DAPT compounds significantly increased β-galactosidase activity and hence misincorporation (Fig. 6). Gentamicin reduces translation fidelity two- to fourfold, depending on the missense codon, while DAPT compounds display an even stronger effect (three- to fivefold).

In summary, in vivo results from translation-dependent bactericidal activity and misincorporation are consistent with a mechanism of action of the DAPT compounds as antibacterials that target the ribosomal decoding site.

In vivo efficacy of DAPT compound 1c. To explore the potential of the DAPT anilide series for the development of novel antibiotics, we tested for in vivo efficacy of 1c against a mouse systemic infection (Fig. 7). Mice that were infected i.p. with a lethal dose of *E. coli* were treated with 1c via the i.v. or i.p. route. A correlation between compound dose and protective effect was observed for i.v. administration of 1c over a range of 5 to 1.25 mg/kg of body weight, suggesting a calculated 50% protective dose of 2.4 mg/kg (Fig. 7). For the i.v. route, 100%

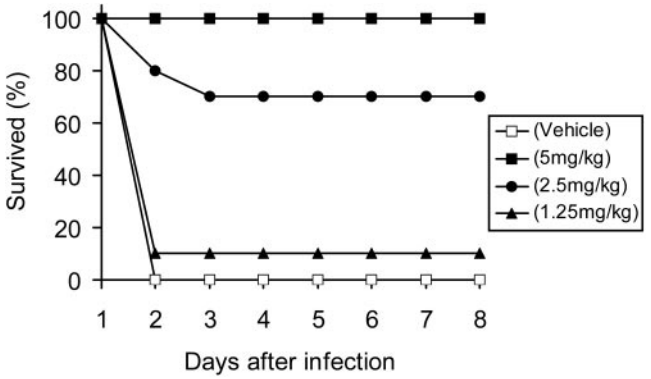

FIG. 7. Efficacy of DAPT compound 1c in a mouse protection model against a lethal dose of *E. coli* ATTC 25922 (for experimental details, see Materials and Methods). A single dose of compound was administered 1 h after inoculation by an i.v. route (at 1.25, 2.5, and 5 mg/kg). The i.v. 50% protective dose was calculated as 2.4 mg/kg. Ten animals were used with each dose level.

protection was achieved by 5 mg/kg of DAPT compound. Two doses (5 and 10 mg/kg) were tested for the i.p. route, both of which resulted in 100% protection (data not shown). All animals survived treatment regimens at the highest concentration levels, without showing signs of acute compound toxicity, independently of the route of administration.

Conclusions and perspective. Our efforts to develop a novel chemical class of antibacterials directed at the ribosome have led to the discovery of the DAPT compounds (31). Biological activity of the DAPT series was improved by using medicinal chemistry and guidance from in vitro testing, eventually yielding lead compounds that were efficacious in vivo. Preliminary characterization of lead compounds suggests a mechanism of action in agreement with the compound design objective, that is, interference with the ribosomal decoding site. Therefore, the DAPT antibacterials represent the first novel class of antibacterials, active in a murine model, that were designed guided by structural information of the bacterial ribosome. Future mechanistic and structural studies could reveal a detailed picture of the interaction of DAPT compounds with the ribosome and provide a basis for further optimization of these novel antibacterials.

ACKNOWLEDGMENTS

This work was supported in part by Public Health Service grant AI51104 to T.H. from the National Institute of Allergy and Infectious Diseases.

We thank D. Averett for helpful suggestions in preparation of the manuscript.

REFERENCES

1. **Auerbach, T., A. Bashan, and A. Yonath.** 2004. Ribosomal antibiotics: structural basis for resistance, synergism and selectivity. Trends Biotechnol. **22:**570–576.
2. **Barluenga, S., K. B. Simonsen, E. S. Littlefield, B. K. Ayida, D. Vourloumis, G. C. Winters, M. Takahashi, S. Shandrick, Q. Zhao, Q. Han, and T. Hermann.** 2004. Rational design of azepane-glycoside antibiotics targeting the bacterial ribosome. Bioorg. Med. Chem. Lett. **14:**713–718.
3. **Brodersen, D. E., W. M. Clemons, A. P. Carter, R. J. Morgan-Warren, B. T. Wimberly, and V. Ramakrishnan.** 2000. The structural basis for the action of the antibiotics tetracycline, pactamycin, and hygromycin B on the 30S ribosomal subunit. Cell **103:**1143–1154.
4. **Carter, A. P., W. M. Clemons, D. Brodersen, R. J. Morgan-Warren, B. T. Wimberly, and V. Ramakrishnan.** 2000. Functional insights from the structure of the 30S ribosomal subunit and its interactions with antibiotics. Nature **407:**340–348.
5. **Cory, A. H., T. C. Owen, J. A. Barltrop, and J. G. Cory.** 1991. Use of an aqueous soluble tetrazolium/formazan assay for cell growth assays in culture. Cancer Commun. **3:**207–212.
6. **Foloppe, N., I. J. Chen, B. Davis, A. Hold, D. Morley, and R. Howes.** 2004. A structure-based strategy to identify new molecular scaffolds targeting the bacterial ribosomal A-site. Bioorg. Med. Chem. **12:**935–947.
7. **Hanessian, S., A. Kornienko, and E. E. Swayze.** 2003. Probing the functional requirements of the L-haba side-chain of amikacin—synthesis, 16S A-site rRNA binding, and antibacterial activity. Tetrahedron **59:**995–1007.
8. **Hermann, T.** 2005. Drugs targeting the ribosome. Curr. Opin. Struct. Biol. **15:**355–366.
9. **Hermann, T., and Y. Tor.** 2005. RNA as a target for small-molecule therapeutics. Expert Opin. Ther. Patents **15:**49–62.
10. **Kaul, M., and D. S. Pilch.** 2002. Thermodynamics of aminoglycoside-rRNA recognition: the binding of neomycin-class aminoglycosides to the A site of 16S rRNA. Biochemistry **41:**7695–7706.
11. **Kaul, M., C. M. Barbieri, J. E. Kerrigan, and D. S. Pilch.** 2003. Coupling of drug protonation to the specific binding of aminoglycosides to the A site of 16S rRNA: elucidation of the number of drug amino groups involved and their identities. J. Mol. Biol. **326:**1373–1387.
12. **Kaul, M., C. M. Barbieri, and D. S. Pilch.** 2004. Fluorescence-based approach for detecting and characterizing antibiotic-induced conformational changes in ribosomal RNA: comparing aminoglycoside binding to prokaryotic and eukaryotic ribosomal RNA sequences. J. Am. Chem. Soc. **126:**3447–3453.
13. **Knowles, D. J. C., N. Foloppe, N. B. Matassova, and A. I. H. Murchie.** 2002. The bacterial ribosome, a promising focus for structure-based drug design. Curr. Opin. Pharmacol. **2:**501–506.
14. **Kotra, L. P., J. Haddad, and S. Mobashery.** 2000. Aminoglycosides: perspectives on mechanisms of action and resistance and strategies to counter resistance. Antimicrob. Agents Chemother. **44:**3249–3256.
15. **Lorian, V.** 1996. Antibiotics in laboratory medicine, 4th ed. Williams & Wilkins, Baltimore, Md.
16. **Miller, J. H.** 1992. A short course in bacterial genetics. Cold Spring Harbor Laboratory Press, Cold Spring Harbor, N.Y.
17. **National Committee for Clinical Laboratory Standards.** 1997. Methods for dilution antimicrobial susceptibility tests for bacteria that grow aerobically. M7-A4. National Committee for Clinical Laboratory Standards, Wayne, Pa.
18. **Ogle, J. M., A. P. Carter, and V. Ramakrishnan.** 2003. Insights into the decoding mechanism from recent ribosome structures. Trends Biochem. Sci. **28:**259–266.
19. **Pilch, D. S., M. Kaul, C. M. Barbieri, and J. E. Kerrigan.** 2003. Thermodynamics of aminoglycoside-rRNA recognition. Biopolymers **70:**58–79.
20. **Shandrick, S., Q. Zhao, Q. Han, B. K. Ayida, M. Takahashi, G. C. Winters, K. B. Simonsen, D. Vourloumis, and T. Hermann.** 2004. Monitoring molecular recognition of the ribosomal decoding site. Angew. Chem. Int. Ed. Engl. **43:**3177–3182.
21. **Simonsen, K. B., B. K. Ayida, D. Vourloumis, M. Takahashi, G. C. Winters, S. Barluenga, S. Qamar, S. Shandrick, Q. Zhao, and T. Hermann.** 2002. Novel paromamine derivatives exploring shallow-groove recognition of ribosomal-decoding-site RNA. Chembiochem **3:**1223–1228.
22. **Simonsen, K. B., B. K. Ayida, D. Vourloumis, G. C. Winters, M. Takahashi, S. Shandrick, Q. Zhao, and T. Hermann.** 2003. Piperidine glycosides targeting the ribosomal decoding site. Chembiochem **4:**886–890.
23. **Thompson, J., M. O'Connor, J. A. Mills, and A. E. Dahlberg.** 2002. The protein synthesis inhibitors, oxazolidinones and chloramphenicol, cause extensive translational inaccuracy *in vivo*. J. Mol. Biol. **322:**273–279.
24. **Vakulenko, S. B., and S. Mobashery.** 2003. Versatility of aminoglycosides and prospects for their future. Clin. Microbiol. Rev. **16:**430–450.
25. **Vicens, Q., and E. Westhof.** 2003. RNA as a drug target: the case of aminoglycosides. Chembiochem **4:**1018–1023.
26. **Vicens, Q., and E. Westhof.** 2003. Molecular recognition of aminoglycoside antibiotics by ribosomal RNA and resistance enzymes: an analysis of X-ray crystal structures. Biopolymers **70:**42–57.
27. **Vourloumis, D., M. Takahashi, G. C. Winters, K. B. Simonsen, B. K. Ayida, S. Barluenga, S. Qamar, S. Shandrick, Q. Zhao, and T. Hermann.** 2002. Novel 2,5-dideoxystreptamine derivatives targeting the ribosomal decoding site RNA. Bioorg. Med. Chem. Lett. **12:**3367–3372.
28. **Vourloumis, D., G. C. Winters, M. Takahashi, K. B. Simonsen, B. K. Ayida, S. Shandrick, Q. Zhao, and T. Hermann.** 2003. Novel acyclic deoxystreptamine mimetics targeting the ribosomal decoding site. Chembiochem **4:**879–885.
29. **Vourloumis, D., G. C. Winters, K. B. Simonsen, M. Takahashi, B. K. Ayida, S. Shandrick, Q. Zhao, Q. Han, and T. Hermann.** 2005. Aminoglycoside-hybrid ligands targeting the ribosomal decoding site. Chembiochem **6:**58–65.
30. **Walsh, C.** 2003. Antibiotics: actions, origins, resistance. ASM Press, Washington, D.C.
31. **Zhou, Y., D. Vourloumis, V. E. Gregor, G. C. Winters, T. Hermann, B. K. Ayida, Z. Sun, D. Murphy, and K. B. Simonsen.** 2005. Antibacterial 3,5-diaminopiperidine-substituted aromatic and heteroaromatic compounds. PCT WO 2005/028467 A1. World Intellectual Property Organization, Geneva, Switzerland.